

Mapping the Isoprenoid Binding Pocket of PDE δ by a Semisynthetic, Photoactivatable N-Ras Lipoprotein

Michael Alexander,^[b] Marc Gerauer,^[a] Markos Pechlivanis,^[b] Boriana Popkirova,^[b] Radovan Dvorsky,^[b] Luc Brunsveld,^[a] Herbert Waldmann,^{*,[a]} and Jürgen Kuhlmann^{†[b]}

Biologically functional Ras isoforms undergo post-translational modifications starting with farnesylation of the most C-terminal cysteine. Combined with further processing steps, this isoprenylation allows for the anchoring of these proteins in endomembranes, where signal transduction events take place. The specific localization is subject to dynamic regulation and assumed to modulate the activity of Ras proteins by governing their spatiotemporal distribution. The δ subunit of phosphodiesterase (PDE δ) has attracted attention as a solubilization factor of isoprenylated Ras. In this study, we demonstrate that critical residues in the

putative isoprenoid pocket of PDE δ can be mapped by coupling with a semisynthetic N-Ras lipoprotein in which the native farnesyl group of the processed protein was replaced by a photoactivatable geranyl benzophenone moiety. The crosslinked product included parts of β -sheet 9 of PDE δ , which contains the highly conserved amino acids V145 and L147. Modeling of the PDE δ -geranyl benzophenone (GerBP) complex supports the conclusion that the photolabeled sequence is embedded in the putative isoprenoid pocket of PDE δ .

Introduction

Members of the Ras family play a crucial role in signal transduction processes involved in cell division or differentiation. In this context, they function as molecular switches—a role that is strictly linked to their location in endogenous membranes.^[1] While earlier concepts presented a more static view, recent studies emphasize that the dynamic translocation of Ras isoforms between different endomembranes spatiotemporally controls their biological activity.^[2] In this view, H-, N-, and K-Ras possess reversible membrane-binding motifs. Both H- and N-Ras are equipped with hydrolysable palmitoyl thioesters, the cleavage of which results in drastic weakening of Ras anchorage in lipid bilayers,^[3] while phosphorylation of a serine in the polybasic stretch of the K-RasB C terminus perturbs the electrostatic interaction with the negatively charged inner leaflet of the plasma membrane.^[4] Farnesylation of the most C-terminal cysteine, which occurs in all Ras isoforms, is the second modification that contributes to membrane association. Due to the stable character of the thioether between the isoprenoid and the protein, farnesyl-binding chaperones might mask this hydrophobic motif for intracellular translocation.^[5]

One candidate for such a farnesyl chaperone is phosphodiesterase δ (PDE δ), which has been described as an interaction partner of isoprenoid-modified small molecules or prenylated proteins in several studies.^[6–11] Over-expression of PDE δ interferes with Ras trafficking; this has led to the idea that PDE δ might be involved in the delivery of prenylated proteins to endomembranes.^[9] However, knowledge about the molecular details of prenyl binding by PDE δ , in particular the amino acids decisive for interaction with Ras, is scarce.

In order to gain insight into the structural requirements for the binding of PDE δ to isoprenylated Ras, we utilized semisynthetic Ras lipoprotein from a bacterially expressed Ras core,

which was ligated to a chemically synthesized lipopeptide at the C terminus.^[12–15] We have shown previously that N-Ras lipoproteins with a geranyl benzophenone (GerBP) modification retain their biological activity in cellular setups.^[16] Their use results in enhanced activity of the exchange factor Sos, as similarly reported for farnesylated Ras.^[17] Substitution of the natural farnesyl with a photoactive GerBP moiety allowed the residues in PDE δ that form the putative isoprenoid binding pocket to be mapped (Figure 1).

Results

Synthesis and ligation


To characterize the putative isoprenyl binding pocket of full length PDE δ , a semisynthetic N-Ras lipoprotein with a photoactivatable group in the farnesyl moiety for crosslinking to

[a] M. Gerauer,⁺ Dr. L. Brunsveld, Prof. Dr. H. Waldmann
Department of Chemical Biology
Max Planck Institute of Molecular Physiology
Otto-Hahn Strasse 11, 44227 Dortmund (Germany)
Fax: (+ 49) 231-1332499
E-mail: herbert.waldmann@mpi-dortmund.mpg.de

[b] M. Alexander,⁺ Dr. M. Pechlivanis, Dr. B. Popkirova, Dr. R. Dvorsky,
Dr. J. Kuhlmann
Department of Structural Biology
Max Planck Institute of Molecular Physiology
Otto-Hahn Strasse 11, 44227 Dortmund (Germany)

[*] These authors contributed equally to this work.

[†] Deceased.

 Supporting information for this article is available on the WWW under <http://www.chembiochem.org> or from the author: analytical data for compounds 1–8, Figures S1–S2, and PyMOL files of Figure 6A–D.

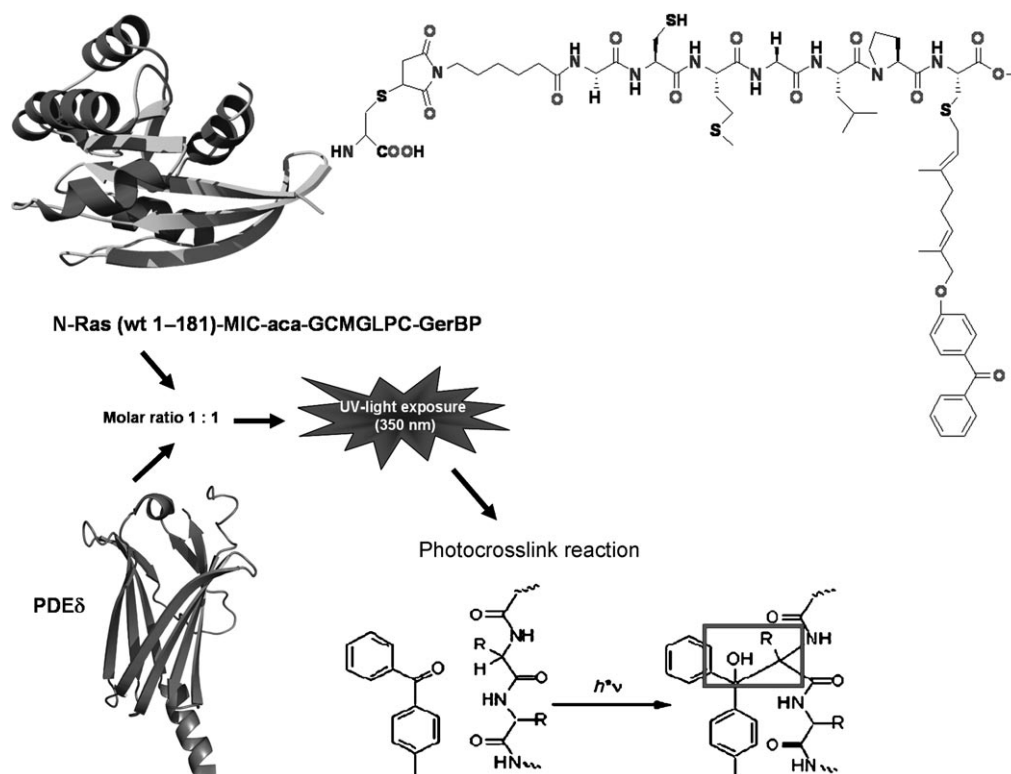
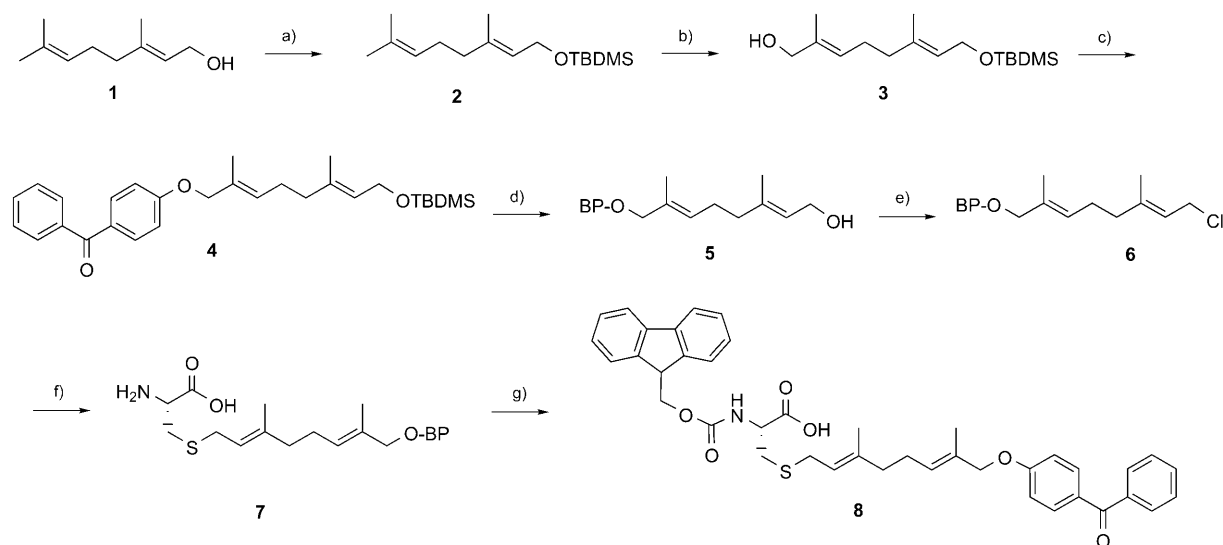


Figure 1. Overview of the crosslinking reaction of semisynthetic wt-N-Ras(1–181)-MIC-aca-GCMGLPC-GerBP-OMe and PDE δ . The N-Ras C terminus was ligated to a chemically synthesized carboxymethylated, lipidated, and chemically tagged (MIC-aca-GCMGLPC-GerBP-OMe) heptapeptide.

PDE δ was required. To this end, a N-Ras(1–181)-MIC-aca-Gly-Cys-Met-Gly-Leu-Pro-Cys(GerBP)-OMe (N-Ras-GerBP) construct was designed and synthesized. In this construct, the natural farnesyl moiety at the carboxymethylated C-terminal cysteine was replaced by a photoactive GerBP residue. In order to as-

semble the C-terminal peptide on the solid phase, a Fmoc-protected cysteine building block (**8**) that incorporated the GerBP residue needed to be generated (Scheme 1). The synthesis followed well-established steps for modification of the geranyl group.^[16,18] The free thiol of unprotected cysteine was alkylated

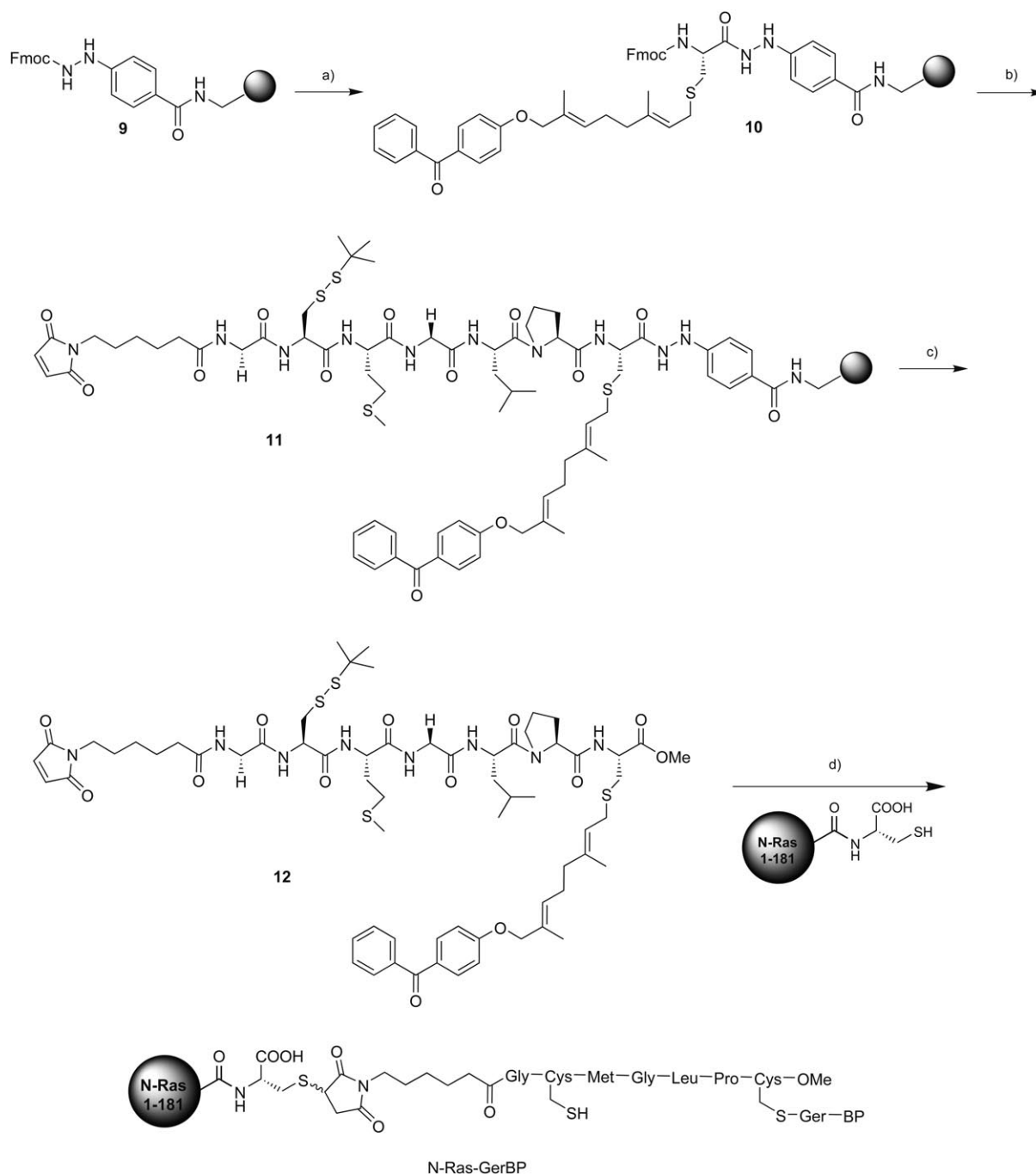


Scheme 1. a) DIPEA (2 equiv), TBDMS (1 equiv) in CH_2Cl_2 , 0°C ; b) SeO_2 (0.1 equiv), $t\text{Bu-OOH}$ (0.1 equiv), salicylic acid (4 equiv) in CH_2Cl_2 , 0°C ; c) P(Ph)_3 (1.5 equiv), DIAD (1.5 equiv), benzophenone (1.2 equiv) in THF, 0°C ; d) TBAF (1.2 equiv) in THF, 0°C ; e) NCS (1.1 equiv), Me_2S (2 equiv) in CH_2Cl_2 , -40°C ; f) NH_3/MeOH (7 M, 16 equiv), Cys-HCl (1.2 equiv) in MeOH, 0°C ; g) Fmoc-OSu (3.2 equiv), Et_3N (3.2 equiv) in CH_2Cl_2 , 20°C .

with geranyl chloride **6**^[18]. The amine functionality of the resulting cysteine derivative, **7**, was Fmoc protected to yield the desired building block **8**. Peptide **12** was assembled from **8** on solid support by using the hydrazine linker (Scheme 2).^[19] Pure peptide **12** was thus obtained in 41% yield. The peptide was subsequently ligated under buffered conditions to the wild-type (wt) N-Ras(1–181) construct, which featured a C-terminal cysteine.^[12–15]

Photocrosslinking and analysis

To shed light on the contribution of the prenyl moiety of N-Ras and its interaction with PDE δ , photocrosslinking (PCL) experiments were performed. A stable crosslinked product of the N-Ras lipoprotein and PDE δ might be expected after photoactivation, if the prenyl moiety directly and specifically interacts with PDE δ . Indeed, a new defined band at 38 kDa was observed in the SDS-PAGE analysis after UV-light exposure of N-



Scheme 2. a) 1: DMF/piperidine (1:1); 2: **8** (4 equiv), HOBt (4 equiv), HBTU (4 equiv), 2,4,6-collidine (4 equiv) in DMF; b) SPPS; deprotection: DMF/piperidine (1:1), coupling: HBTU (4 equiv), HOBt (4 equiv), Fmoc-AA-OH (4 equiv), DIPEA (8 equiv) in DMF; c) Cu(OAc)₂ (0.55 equiv), pyridine (35 equiv), MeOH (215 equiv) in CH₂Cl₂; d) buffered solution of 11% Triton X-114 (20 equiv), 30 mM Tris-HCl, 100 mM NaCl (1 mL), 4 °C.

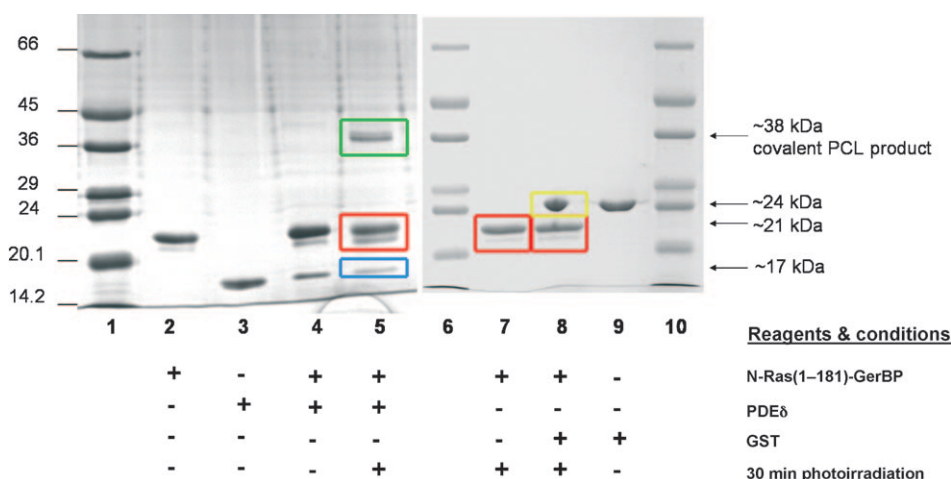


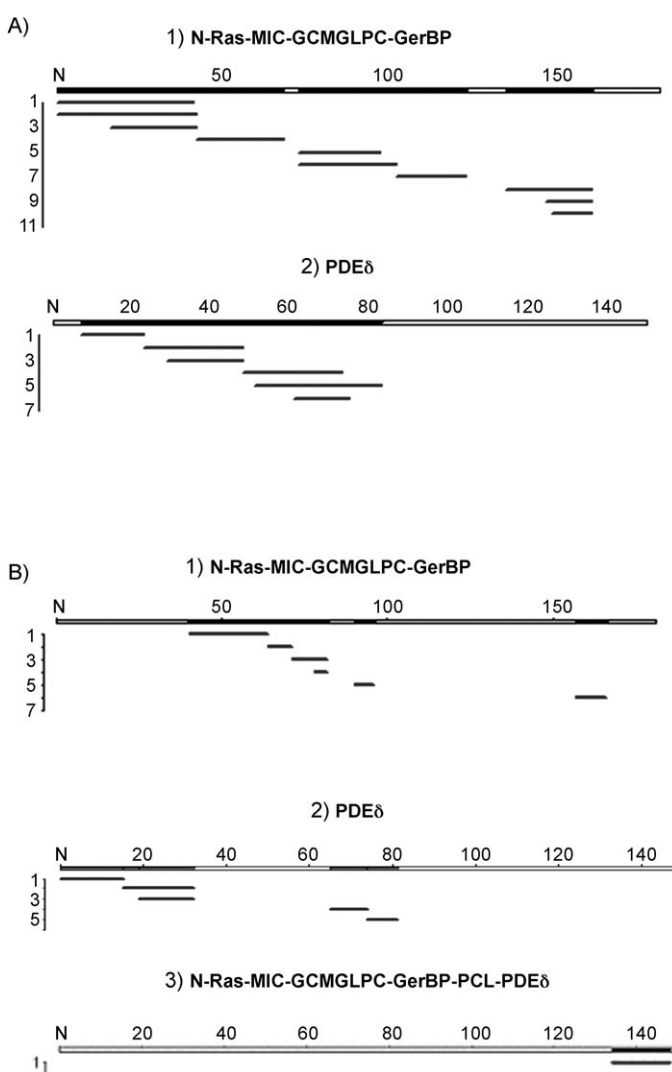
Figure 2. SDS-PAGE analysis of the photocrosslinking (PCL) reaction. Lanes 1, 6, 10: protein marker (SDS-7); lane 2: N-Ras(1-181)-GerBP; lane 3: PDE δ ; lane 4: reaction mixture before photoirradiation; lane 5: sample after 30 min of photoirradiation. Green box: PCL product (38 kDa); red and blue boxes: starting materials; lane 7: N-Ras(1-181)-GerBP alone, and lane 8: in the presence of GST (24 kDa, yellow box) after UV exposure. Lane 9: GST.

Ras-GerBP and PDE δ (Figure 2). This band had the expected mass of the coupled product of N-Ras-GerBP (21 kDa) and PDE δ (17 kDa). The amount of both starting proteins decreased compared to the bands in the unexposed sample (Figure 2, lane 4 vs. lane 5). The lower (less intense) band of N-Ras-GerBP represents about 10% uncoupled N-Ras(1-181) as confirmed by SDS-PAGE analysis and mass spectrometry (Figure S1 in the Supporting Information). The intensity of this band was not attenuated compared to the unexposed sample; this demonstrates the necessity of GerBP for the reaction. As a control for the specificity of photoproduct formation, an additional cross-linking experiment with N-Ras-GerBP and GST, which is a non-Ras-binding reaction partner, was performed (Figure 2, lanes 7-9). When using identical protein concentrations and PCL conditions, no N-Ras-GST crosslink product was observed. Furthermore, no PCL products were identified after illumination of a pure N-Ras-MIC-GerBP solution. PCL N-Ras-GerBP-PDE δ was separated from the starting proteins by gel filtration and analyzed by silver staining after SDS-PAGE (Figure S2).

After purification, the PCL product was proteolytically cleaved with trypsin and chymotrypsin for at least 12 h at 37 °C (trypsin) and 25 °C (chymotrypsin). Mass spectrometric analysis was performed by MALDI-TOF-MS after proteolytic digestion and conditioning of the peptide mixture. Products of proteolysis were identified with PAWS software by taking into consideration the specific digestion conditions and factors,

Figure 3. MS analysis of the crosslinking product of PDE δ and N-Ras-GerBP. After gel filtration the PCL product was cleaved with either trypsin or chymotrypsin for 12 h. Resulting fragments were analyzed by MALDI-TOF-MS after disulfide bond reduction with DTE and alkylation with IAA. All signals were verified by using PAWS software, which assumed specific theoretical protease cleavage sites, and modifications, such as miscleavage, alkylation, etc. A) Results from trypsin digestion; fragments attributed to 1) N-Ras, 2) PDE δ . B) Results from chymotrypsin digestion; fragments attributed to 1) N-Ras, 2) PDE δ , 3) photocrosslinked products.

such as carboxymethylation and miscleavage. Sequence coverage of up to 79% for N-Ras-GerBP and 45% for PDE δ could be achieved after trypsin digestion. However, a distinct fragment for a crosslinked product of PDE δ with the N-Ras-MIC-GerBP C terminus could not be assigned (Figure 3A). The sequence coverage after digestion with chymotrypsin was 33.7% for the N-Ras-GerBP and 23.3% for the PDE δ sequence (Figure 3B), again without direct correlation of a putative cross-link fragment. Controls without protein revealed no peptide fragments due to potential autodigestion of the proteases applied (data not shown); this indicates that all peptides detect-



ed in the digestion reactions originated from the crosslinked product.

Analytical mass spectrometry of the isolated MIC-ac-GCMGLPC-GerBP-OMe lipopeptide **12** yielded relevant information for the correct assignment of the unassigned signals in the peptide mixture obtained after PCL. ESI-MS of **12** revealed nonenzymatic breakage of the lipopeptide between leucine and proline (Figure 4B), which resulted in a PC-GerBP-OMe fragment with an apparent mass of 565.22 Da (565.27 Da for the calculated monoisotopic mass). Reanalysis of the original data for the presence of putative coupling products, which included the PC-GerBP-OMe fragment after the mass-induced leucine–proline break, revealed a signal at 2201.35 Da in the chymotrypsin digested PCL sample (Figure 4A). This fragment could be attributed to the covalent linkage of the PC-GerBP-OMe fragment with a C-terminal peptide fragment of PDE δ (D135–F148), which contributed an additional mass of 1635.8 Da. The fragment was unambiguously identified in independent experiments by MALDI-TOF-MS. A scheme for the formation of the coupling fragment and the PDE δ secondary structure is given in Figure 5.

In silico evaluation

To support the findings of the PCL studies with a molecular model, the GerBP residue was docked in silico into the farnesyl binding pocket of PDE δ . First attempts to find a binding mode of GerBP within the hydrophobic pocket of the ArL2-GTP–PDE δ crystal structure^[8] were unsuccessful. The putative isoprenoid binding pocket of PDE δ , when compared to the geranylgeranyl (GerGer) moiety in the RhoGDI–Cdc42*GDP complex,^[20] is smaller than in RhoGDI. Crucial residues in PDE δ that restrict the binding pocket for a farnesyl or GerBP residue are M20 and I129, respectively. For this reason we introduced a ~ 2.5 Å conformational shift for I129 in silico, towards a position that corresponds to the structural orientation of the analogous residue I177 of RhoGDI in the RhoGDI–Cdc42 complex. Furthermore, the position of M20 was rearranged by ~ 2.5 Å so that its sulfur atom did not point into the binding pocket. I129 is conserved between RhoGDI and PDE δ and the corresponding I177 in RhoGDI is located in the hydrophobic pocket of the GDI approximately in the center of the GerGer chain.^[20] The highest ranking solutions from docking of flexible GerBP into the al-

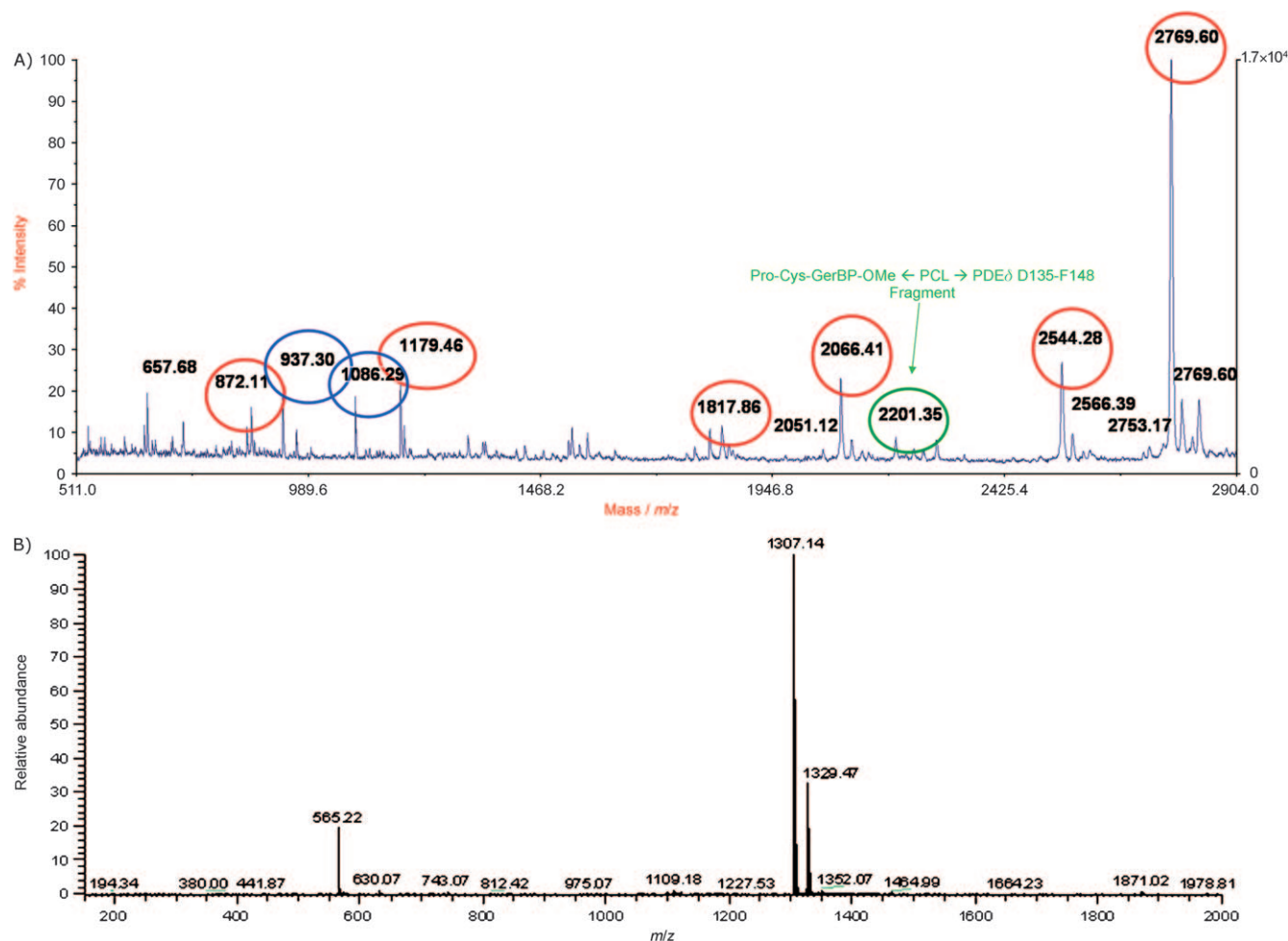


Figure 4. MS analysis of the crosslinked product. A) Chymotrypsin digestion of the product resulted in a fragment with a monoisotopic mass of 2201.35 Da ($[M+H]^+$) in the MALDI-TOF analysis, which could be attributed to a PDE δ peptide with amino acids D135–F148 coupled to Pro-Cys-GerBP-OMe. The masses in red belong to fragments of the N-Ras–GerBP and in blue to PDE δ . B) A corresponding specific nonenzymatic fragmentation was observed for the MIC-GCMGLPC–GerBP peptide **12**, which showed a break of the fragment at the N terminus of proline with a monoisotopic mass of 565.22 Da ($[M+H]^+$) in an ESI spectrum.

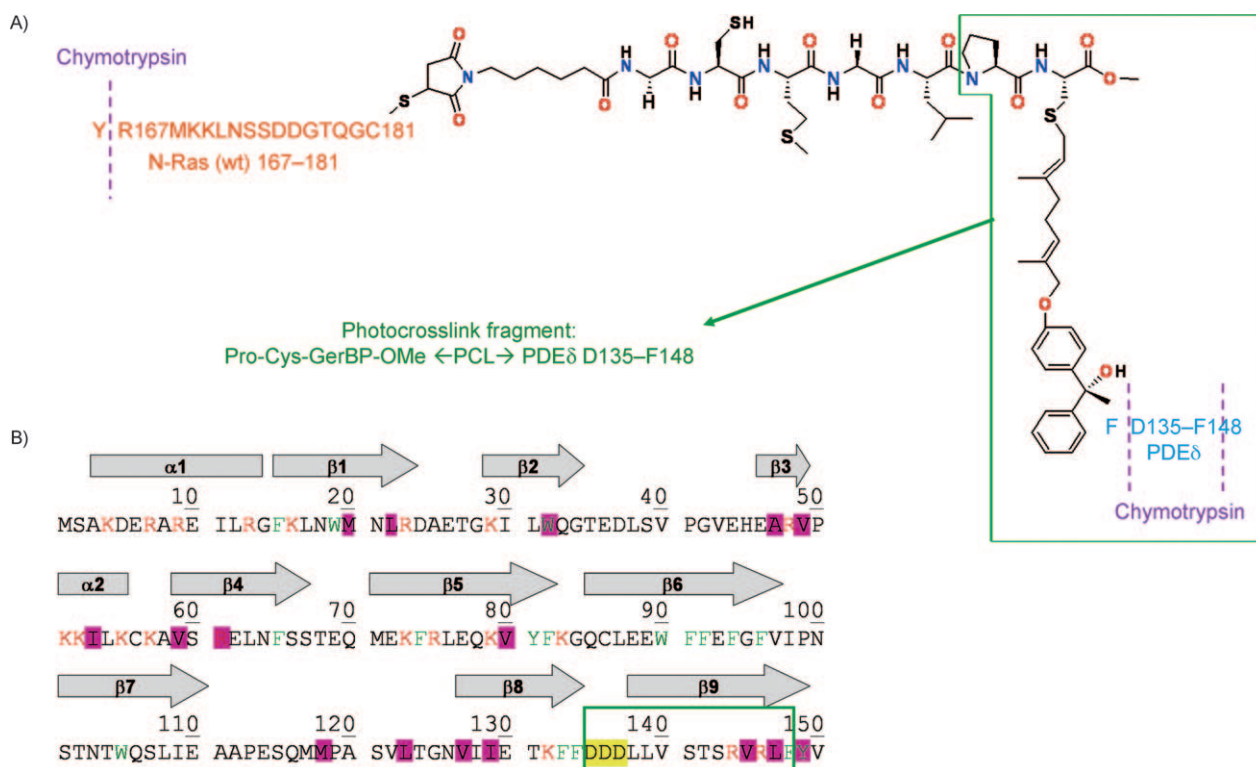


Figure 5. A) Sequence of the N-Ras–GerBP–PDE δ fragment identified by MALDI-TOF MS after crosslinking and proteolytic cleavage with chymotrypsin. B) Sequence and secondary structure of PDE δ crystal form 2.^[8] Red- and green-colored amino acids represent trypsin and chymotrypsin cleavage sites, respectively. Hydrophobic amino acids (highlighted in purple) form the hydrophobic pocket of PDE δ . The aspartates marked in yellow are conserved between PDE δ and all RhoGDI.

tered PDE δ structure resulted in only one strictly defined binding mode (Figures 6A–C). In the final step the PDE δ structure was allowed to relax during energy minimization, while the docked GerBP structure with the highest score value of the previous calculation remained fixed. The nine best ranked binding modes from docking of GerBP to relaxed PDE δ with scoring values comparable to the best solutions from the previous docking run resulted in two distinct final binding modes. They were similar to the previous mode with the carbonyl group of GerBP pointing in the same direction. Residues in the neighborhood of the benzophenone carbonyl included M20, W32, A47, I129, V145, and L147. V145 and L147 were oriented towards the GerBP residue (Figure 6) and in particular faced the benzophenone carbonyl, which is part of the C–C crosslink after photoreaction. Interestingly, a closer look at the pocket structure with the best score revealed that the two hydrophobic residues, V145 and L147 (Figures 6B–C), are in a close enough proximity to crosslink with the activated benzophenone group. Both amino acids are located at the C terminus of PDE δ . The shortest distances between the side chains of V145 and L147 on the one side and the carbonyl of the benzophenone molecule on the other are 3.4 Å and 3.1 Å, respectively. The orientation and the short distances between the two hydrophobic amino acids and the crosslinking ability of benzophenone allow formation of covalent bonds during the photoreaction and support the experimental results. Further putative candidates for prenyl binding and crosslinking are located in

the β -sheets 2, 3, and 8 of PDE δ (W32 4.3 Å, A47 3.6 Å, I129 4.1 Å; Figure 6B), but were not identified with their corresponding fragments in the mass spectrometric analysis. Furthermore, successful docking of a farnesyl group to a relaxed structure of PDE δ showed that the farnesyl binding mode (Figure 6D) is similar to the binding mode of GerBP, although more flexible due to the smaller molecular volume.

Discussion

The PDE δ fragment D135–F148 crosslinked by the photoactivated benzophenone consisted of 14 C-terminal amino acids including three conserved aspartates (D135, D136, D137) involved in the interaction of RhoGDI and Cdc42, which are surprisingly conserved between PDE δ and all RhoGDIs. This acidic stretch plays an important role in stabilizing the interaction of the amino-terminal helix–loop–helix region of RhoGDI and the switch II domain of Cdc42.^[20] The prenyl binding pocket of PDE δ is highly conserved in nature. The amino acid sequence of the frog homologue of mammalian PDE δ was aligned and compared with nine vertebrate and six invertebrate species.^[21] Conserved hydrophobic amino acids contribute to the pocket and form favorable van der Waals contacts along the length of the prenyl group (Figure 6). Thirteen out of sixteen residues of the hydrophobic cavity are identical in at least 14 of the 15 species compared. The PDE δ structure features an immunoglobulin-like β -sandwich fold with two β sheets packed against

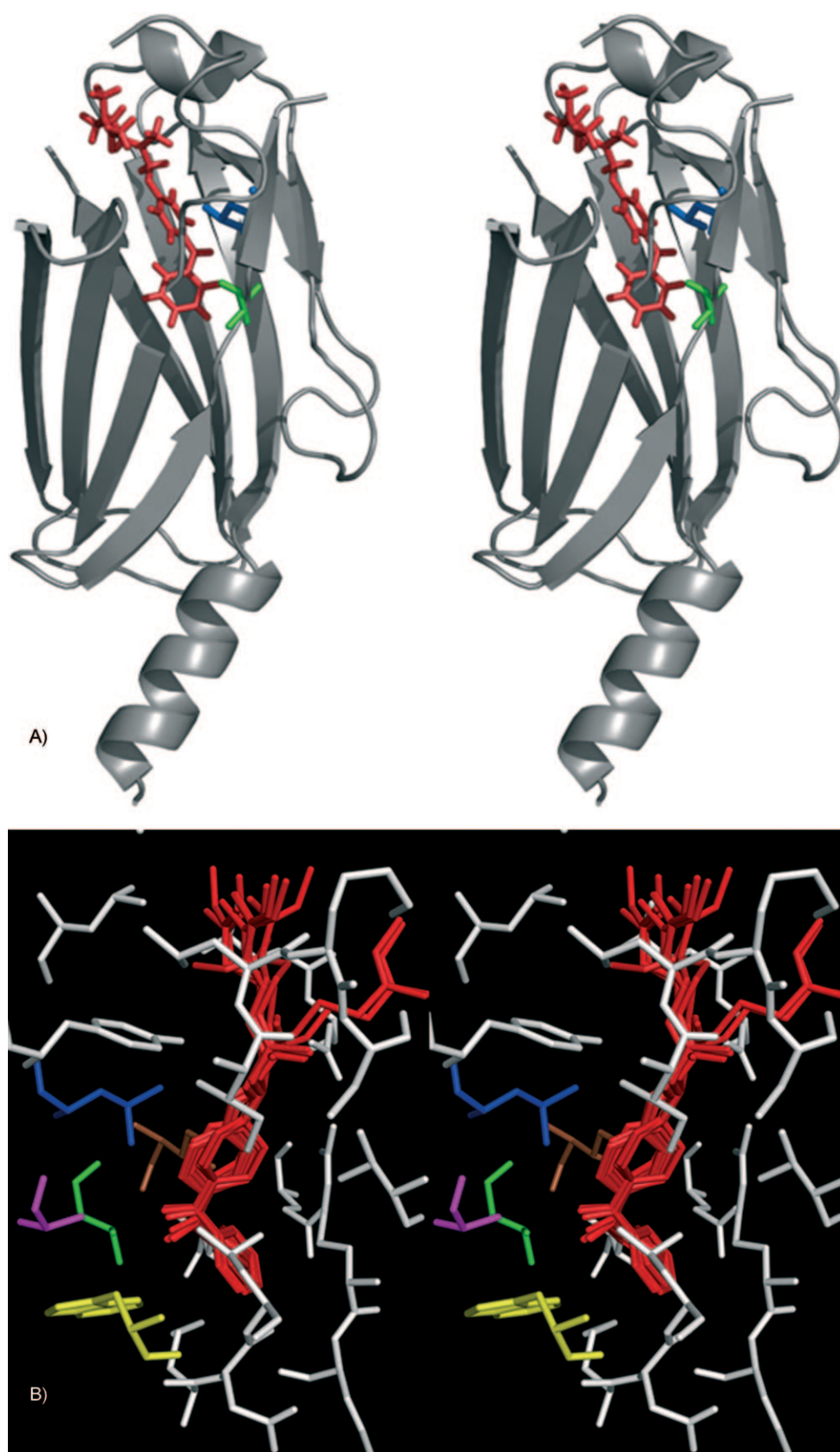


Figure 6. In silico docking of GerBP to the putative binding site of PDE δ (stereo representations). A) Binding of a flexible GerBP group (red sticks), within the rearranged structure of PDE δ (gray ribbon model). Hydrophobic residues V145 and L147 of PDE δ are in green and in blue, respectively. B) Nine best scored docked GerBP groups in the pocket of relaxed PDE δ . Additional residues of the pocket that contact GerBP are showed in purple (A47), yellow (W32), and brown (I129). C) Distances (indicated in Å) from the benzophenone carbonyl of the best scored binding mode of GerBP to the closest methyl residues. D) Result of farnesyl residue (red sticks) docked to the relaxed PDE δ structure.

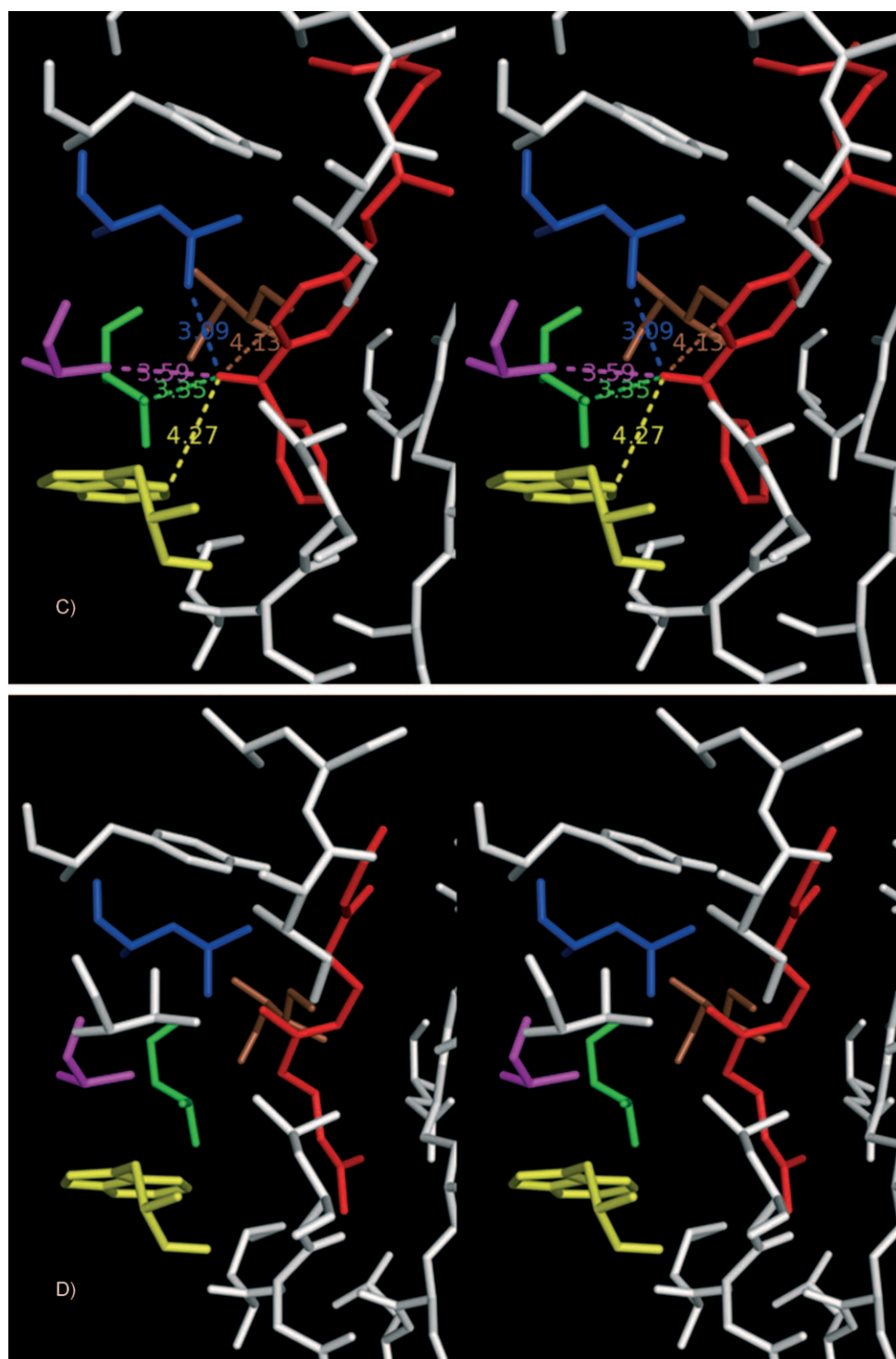


Figure 6. (Continued)

each other ($\beta 1$, $\beta 2$, $\beta 4$, $\beta 7$, and $\beta 3$, $\beta 5$, $\beta 6$, $\beta 8$, $\beta 9$), which is preceded by an N-terminal α helix (α_1). Only a short 3_{10} helix is located in one of the loop regions. RhoGDIs and PDE δ differ in their N-terminal regions.^[8] In particular, the short 3_{10} helix of PDE δ might be responsible for the interaction with Ras proteins.

The PCL PDE δ fragment identified in our study includes two of the conserved hydrophobic residues, V145 and L147. These

residues correspond to the amino acids W194 and L196 in RhoGDI, which belong to the so called “hydrophobic triad” (W194, L77, and F102) or are involved in hydrophobic contacts (L196) with the prenyl residue in RhoGDI.^[8,22] Our *in silico* docking supports the idea that the orientation of the functional carbonyl group of the GerBP for PCL is oriented towards the amino acids in PDE δ that are putatively crosslinked in the coupling fragment identified (L147 and V145; Figures 5A–C). The

corresponding residues L196 and W194 in RhoGDI are both involved in hydrophobic contacts with the GerGer residue of Cdc42 in the binary complex.^[20] The docking of the farnesyl group indicates that PDE δ is able to anchor naturally modified Ras (Figure 6D) in a conformational and positional mode very similar to bound Ras–GerBP.

Conclusions

Several studies have identified β -barrel shaped PDE δ as an interaction partner for isoprenoid-modified proteins and peptides.^[8–10] It has also been observed that PDE δ binds prenyl side chains (farnesyl and GerGer groups) with a stoichiometry of 1:1.^[11] However, the exact organization of the interface between the immunoglobulin-like PDE δ and the isoprene side chain of a binding partner have not been characterized yet. The crystal structure of PDE δ ^[8] revealed a β -propeller structure with a shape very similar to that seen for RhoGDI in complex with Cdc42,^[20] but the putative PDE δ prenyl binding pocket was significantly shorter than the RhoGDI GerGer binding structure. Over-expression of PDE δ results in increase of the cytosolic pool of both Ras and Rho proteins^[9] and further small GTPases. Beside Ras, Rab13, Rap, and Rho6 were identified to interact with PDE δ .^[6,10,23] Therefore, PDE δ was suggested to be a solubilization factor for Ras proteins.

In this study, we confirmed that the hydrophobic pocket visible in the PDE δ structure is indeed involved in the specific recognition of farnesylated proteins. For this purpose, a semi-synthetic N-Ras lipoprotein containing a carboxymethylated and isoprenylated C-terminal cysteine was utilized, and the last isoprene monomer of the natural farnesyl was replaced by a benzophenone moiety. The resulting GerBP modification was accepted as a functional substitution for the farnesyl side chain in both protein interactions^[17] and cellular signaling^[16] and is a well-suited tool for mapping isoprene-sensitive proteins. The farnesyl binding pocket of PDE δ was mapped through application of a Ras lipoprotein with a photoactivatable functionality in the isoprenoid residue. This approach can be extended to other isoprenoid-sensitive binding partners of Ras and other post-translationally farnesylated or geranylgeranylated proteins. Moreover, benzophenone-modified baits are promising tools for cellular photolabeling studies since they are chemically stable and their activation (350–360 nm) does not damage proteins.^[24–26] Future investigations, therefore, can address yet unidentified membrane-embedded binding partners of Ras proteins that might regulate localization of the small GTPase in heterogenous membrane compartments.^[27]

Experimental Section

Protein expression, purification, and synthesis of lipoproteins: Generation of semisynthetic lipoproteins has been described in detail before.^[28] For the photoactivatable N-Ras construct, the heptapeptide MIC-GC(StBu)MGLPC-GerBP-OMe, which mimics the N-Ras C terminus, was utilized.^[17]

Full-length PDE δ cDNA was subcloned into the pProEx-HTb vector by using BamHI–EcoRI restriction sites. The expression construct in-

cludes an N-terminal His-tag followed by a Tev-cleavage site. The plasmid coding for N-terminal His-tagged full-length PDE δ was sequenced to determine correct fragment boundaries and then transformed into the *Escherichia coli* strain BL21-CodonPlus-(DE3)-RIL (Stratagene). Culture and expression was performed in LB medium containing ampicillin (100 mg L⁻¹) and incubation at 37 °C. Expression was induced with IPTG (isopropyl- β -D-thiogalactopyranoside; 250 μ M) at a cell density absorbance of A_{600} 0.6, and incubation was continued at 20 °C, overnight. Bacteria pellets were resuspended in Tris-HCl (50 mM, pH 7.4), NaCl (150 mM), glycerol (10%, v/v), β -mercaptoethanol (2 mM). PMSF (phenylmethylsulfonyl fluoride; up to 1 mM) and DNase I (0.5 mg) were added, and the cells were lysed by using a microfluidizer (Microfluidics). Cell debris was removed by centrifugation and clear supernatant was loaded onto a Ni²⁺-NTA column (25 mL of Ni²⁺-NTA resin; Qiagen) after centrifugation for 30 min at 30 000 g. The column was pre-equilibrated with the buffer, as described above, with additional imidazole (30 mM, pH 7.4). After purification with ten column volumes of buffer, elution of His-tag–PDE δ protein was performed by using a linear gradient from 30 to 150 mM imidazole over eight column volumes. His–PDE δ -containing fractions were identified by SDS-PAGE, pooled, and concentrated with amicon ultra microcons (Millipore, Bedford, MA, USA) at 4000 g. His–PDE δ was dialyzed against Tris-HCl (50 mM, pH 7.4), NaCl (150 mM), glycerol (10%, v/v), β -mercaptoethanol (2 mM), and the N-terminal His-tag was cleaved with Tev protease (1 μ g Tev: 500 μ g protein) by incubation at 4 °C for 14 h. PDE δ was depleted of the protease and uncleaved fragments by a second round of Ni²⁺-NTA affinity chromatography. The protein-containing flow-through was concentrated in amicon ultra microcons (M_w CO 10 000) in Tris-HCl (50 mM, pH 7.4), NaCl (150 mM), glycerol (10%, v/v), and β -mercaptoethanol (2 mM).

All protein masses were checked by MALDI mass spectrometry. All purification steps were carried out at 4 °C. Purified protein was stored at –80 °C. Protein concentration were determined by using the Bradford assay.

General procedure for the synthesis of lipidated and labeled peptides: Commercially available Fmoc-4-hydrazinobenzoyl Nova-Gel resin was used for solid-phase reactions. Anhydrous solvents were used for each reaction. The reaction flask (50 mL) had a frit at the bottom, a stopcock to permit rapid filtration and washing of the resin, and a side arm to allow access to the supply of argon. Resin loading was determined by measuring the Fmoc-groups. All amino acids were coupled by using HBTU/HOBt chemistry. Typically, the Fmoc-amino acid (AA; 4 equiv) was treated for two minutes with HBTU (4 equiv), HOBt (4 equiv) in DMF, then DIPEA (8 equiv) was added and stirred for two more minutes. Finally, the solution was added to the resin, which was then agitated for 2–3 h at room temperature. The completeness of the reaction was monitored by the bromophenolblue-test. The Fmoc group was removed by commercially available redistilled piperidine in anhydrous DMF (DMF/piperidine, 1:1; 3 times 5 min). Then the resin was washed five times with DMF, and the next coupling was carried out. Cysteine building blocks were coupled by using HBTU/HOBt/Collidine (4:4:4) in CH₂Cl₂/DMF (1:1). The last step was incorporation of the 6-maleimidohexanoic acid. After Fmoc removal, it was coupled by using HBTU/HOBt/DIPEA (4:4:8). The cleavage of the peptide was carried out by washing the resin three times with anhydrous CH₂Cl₂ and then adding a cocktail of Cu(OAc)₂ (0.55 equiv), pyridine (35 equiv), and MeOH (215 equiv) in anhydrous CH₂Cl₂. The mixture was agitated for 2.5 h, and the resin was washed 5 times with CH₂Cl₂. After washing the organic layer with water, the final pep-

tide was purified by normal phase chromatography (CH₂Cl₂/MeOH, 5%) and obtained in pure form in 41% yield.

Photocrosslinking (PCL) procedure: Before incubation and PCL with PDE δ , the *StBu*-protection group of wt-N-Ras(1–181)-MIC-GC-(*StBu*)MGLPC-GerBP-OMe was reduced and deprotected with DTE (50 mM) by incubation for up to 16 h at 4 °C on a rotary shaker. Afterwards DTE was removed by using HiTrap™-desalting column.

The PCL reaction was performed in NH₄HCO₃ (50 mM), CaCl₂ (10 mM, pH 8.0). PDE δ and the semisynthetic N-Ras lipoprotein were incubated for 2 h at 4 °C (shaker) followed by illumination in a photoreaction chamber (Rayonet RPR-100, Connecticut, USA) with UV-light exposure (350 nm) by using central adjusted quartz photochemical reaction vessels. The total power consumption of eight UV lamps was approximately 200 W. The maximum time frame for the photoreaction did not exceed 30 min at 4 °C. Proteins were applied in a 1:1 ratio and a total volume of 0.1 mL (concentration 50 μ M for each protein).

PCL products and reactants were separated by gel filtration in coupling buffer with a multicomponent Waters 626 LC system on a 10/30 HiLoad Superdex 75 column at a flow rate of 0.5 mL min^{−1}. The column was calibrated with dextran blue (Sigma) for the void volume and the protein standards thyroglobulin (670 kDa), bovine γ -globulin (158 kDa), chicken ovalbumin (44 kDa), equine myoglobin (17.8 kDa), and vitamin B12 (1.35 kDa, all standards from Biosil2000, Bio-Rad). Furthermore, the educts N-Ras(1–181)-MIC-GCMGLPC-GerBP-OMe and PDE δ were applied as pure compounds (50 μ M, 100 μ L) and finally the reaction mixture after crosslinking was separated (N-Ras and PDE δ with 50 μ M starting concentration each, 100 μ L injection volume). Protein-containing fractions were identified by SDS-PAGE and silver staining. Fractions with purified PCL product were pooled, concentrated by acetone precipitation, then resolved in coupling buffer, and used for protease digestion and mass spectrometry.

Proteolytic digestion of PCL products: Purified PCL products were digested in solution with serine endopeptidases (trypsin proteomics grade and chymotrypsin sequencing grade; Roche). Digestion was performed as follows in coupling buffer. First, cysteine–cysteine bonds of proteins were reduced by addition of DTE (final concentration 10 mM) and incubation at 50 °C for 30 min. After being cooled to room temperature, the reduced cysteine sulfides were alkylated with iodacetamide (IAA, final concentration 180 mM) for 20 min at room temperature in the dark. This step prevents the cysteine residues from oxidation and recombining to disulfide bonds. Stable *S*-carboxyamidomethyl derivatives were formed.

Trypsin was activated in HCl (1 mM) and diluted by addition of coupling buffer immediately prior to addition to samples. Incubation with trypsin was done at 37 °C for at least 12 h. Chymotrypsin was activated and diluted by addition of coupling buffer immediately prior to addition to samples. Incubation with chymotrypsin was performed at 25 °C for at least 12 h.

Working concentrations of enzymes were 1/200 to 1/20 of the quantity of protein by weight.

Mass spectrometrical analysis: Protein fragments after protease digestion were subject for the subsequent MALDI-TOF-MS analysis in a Voyager-DE™ MALDI-TOF-MS PRO BioSpectrometry™ workstation (PerSeptive, Applied Biosystems) with delayed extraction^[29,30] and a nitrogen laser (337.1 nm) in the linear mode. External mass calibration typically resulted in ~1.0 Da mass tolerance on the MS;

this allowed for the unequivocal assignment of a high percentage of the proteolytic fragments.

HPLC-ESI-MS spectra for MIC-GCMGLPC-GerBP-OMe were recorded by using a Finnegan LCQ spectrometer (Advantage MAX) connected to a Hewlett-Packard HPLC system equipped with a column changer. Analytical C4 reversed-phase columns (Macherey–Nagel) were used (CC250/4 Nucleosil 120–5C4; flow rate 1.0 mL min^{−1}; solvent A, 0.1% HCOOH in H₂O; solvent B, 0.1% HCOOH in MeOH; gradient program, 20% B (0 min), 20% B (2 min), 90% B (30 min), 95% B (37 min), 20% B (38 min), 20% B (45 min)).

Sequences of human full-length PDE δ and wt-N-Ras(1–181) were subjected to a theoretical protease digestion with the enzymes used in this study (trypsin: C-terminal cleavage of R and K; chymotrypsin: C-terminal cleavage of F, W, and Y). Comparison of the peptide masses found in the mass spectrum with the theoretically expected masses after digestion of both used proteins was performed with PAWS coverage analysis (Protein Analysis Work Sheet; Genomic Solutions, Inc.). Fragment matches and distributions were allowed for mass analysis by PAWS under different factors like miscleavage, alkylation (carbamidomethylation of C), and protease resistant cleavage sides (trypsin: K–P). Unexpected mass fragments, for example, nonenzymatic breaks (C-terminal proline breaks) could not be identified automatically by the proteomics software, but were analyzed manually.

In silico docking and modeling of a GerBP binding site in PDE δ :

The putative isoprenoid binding site in PDE δ was assumed to be on the base of the crystal structure of PDE δ (PDB ID: 1KSH)^[8] superposed on the RhoGDI structure alone (PDB ID: 1KMT)^[31] and in complex with Cdc42 (PDB ID: 1DOA).^[20] The latter was solved with the GerGer side chain of Cdc42 bound in the hydrophobic pocket of RhoGDI. Structural rearrangements in the PDE δ structure were introduced manually by using the program Maestro (Maestro, version 7.5; Schrödinger, LCC, New York, NY, 2006). The structure of the GerBP moiety was generated with the help of build model of Maestro. Docking of the flexible GerBP into the hydrophobic pocket of the fixed PDE δ structure was performed by the program Glide (Glide, version 4.0; Schrödinger, LCC, New York, NY, 2005) by using the default parameter. To ensure that the benzophenone moiety is bound to the pocket, positional constrain of 8.0 Å between the hydroxyl oxygen of T131 and the terminal phenyl ring was applied. Relaxation of PDE δ with bound GerBP was done by the minimization of complex energy in the program MacroModel (Glide, version 9.1; Schrödinger, LCC, New York, NY, 2005). Final analysis of the calculated PDE δ –GerBP complexes as well as the distance analysis between incorporated GerBP and crosslinked residues for design of structural pictures was done in PyMOL™ (<http://pymol.sourceforge.net/>).

Acknowledgements

We thank Fred Wittinghofer for continuous support and discussion. Christine Nowak is acknowledged for excellent technical assistance. This work was supported by the Max-Planck Gesellschaft (MPG), the Sonderforschungsbereich (SFB) 642 “GTP- and ATP-dependent membrane processes”, by the European Union (Europäischer Fond für regionale Entwicklung) the state of Northrhine–Westphalia, and by a Sofja Kovalevskaja Award of the Alexander von Humboldt Foundation and the BMBF to L.B.

Keywords: farnesyl group • N-Ras • PDE δ • photoaffinity labeling • proteomics

- [1] M. Pechlivanis, J. Kuhlmann, *Biochim. Biophys. Acta, Proteins Proteomics* **2006**, 1764, 1914–1931.
- [2] O. Rocks, A. Peyker, M. Kahms, P. J. Verveer, C. Koerner, M. Lumbierres, J. Kuhlmann, H. Waldmann, A. Wittinghofer P. I. H. Bastiaens, *Science* **2005**, 307, 1746–1752.
- [3] S. Shahinian, J. R. Silvius, *Biochemistry* **1995**, 34, 3813–3822.
- [4] T. G. Bivona, S. E. Quatela, B. O. Bodemann, I. M. Ahearn, M. J. Soskis, A. Mor, J. Miura, H. H. Wiener, L. Wright, S. G. Saba, D. Yim, A. Fein, d. C. Perez, C. Li, C. B. Thompson, A. D. Cox, M. R. Philips, *Mol. Cell* **2006**, 21, 481–493.
- [5] D. Meder, K. Simons, *Science* **2005**, 307, 1731–1733.
- [6] A. M. Marzesco, T. Galli, D. Louvard, A. Zahraoui, *J. Biol. Chem.* **1998**, 273, 22340–22345.
- [7] A. M. Marzesco, T. Galli, D. Louvard, A. Zahraoui, *Regul. Eff. Small GTPases, Part E, 2001* **2001**, 329, 197–209.
- [8] M. Hanzal-Bayer, L. Renault, P. Roversi, A. Wittinghofer, R. C. Hillig, *EMBO J.* **2002**, 21, 2095–2106.
- [9] V. Nancy, I. Callebaut, A. El Marjou, J. de Gunzburg, *J. Biol. Chem.* **2002**, 277, 15076–15084.
- [10] H. Zhang, X.-H. Liu, K. Zhang, K. Chen, J. M. Frederick, G. D. Prestwich, W. Baehr, *J. Biol. Chem.* **2004**, 279, 407–413.
- [11] H. Zhang, S. Hosier, J. M. Terew, K. Zhang, R. H. Cote, W. Baehr, *Methods Enzymol.* **2005**, 403, 42–56.
- [12] B. Bader, K. Kuhn, D. J. Owen, H. Waldmann, A. Wittinghofer, J. Kuhlmann, *Nature* **2000**, 403, 223–226.
- [13] R. Reents, M. Wagner, S. Schlummer, J. Kuhlmann, H. Waldmann H, *ChemBioChem* **2005**, 6, 86–94.
- [14] L. Brunsveld, J. Kuhlmann, K. Alexandrov, A. Wittinghofer, R. S. Goody, H. Waldmann, *Angew. Chem.* **2006**, 118, 6774–6798; *Angew. Chem. Int. Ed.* **2006**, 45, 6622–6646.
- [15] L. Brunsveld, J. Kuhlmann, H. Waldmann H, *Methods* **2006**, 40, 151–165.
- [16] J. Kuhlmann, A. Tebbe, M. Volkert, M. Wagner, K. Uwai, H. Waldmann, *Angew. Chem.* **2002**, 114, 2655–2658; *Angew. Chem. Int. Ed.* **2002**, 41, 2546–2550.
- [17] M. Völkert, K. Uwai, A. Tebbe, B. Popkova, M. Wagner, J. Kuhlmann, H. Waldmann, *J. Am. Chem. Soc.* **2003**, 125, 12749–12758.
- [18] D. M. Marecak, Y. Horiuchi, H. Arai, M. Shimonaga, Y. Maki, T. Koyama, K. Ogura, G. D. Prestwich, *Bioorg. Med. Chem. Lett.* **1997**, 7, 1973–1978.
- [19] M. Lumbierres, J. M. Palomo, G. Kragol, S. Roehrs, O. Müller, H. Waldmann, *Chem. Eur. J.* **2005**, 11, 7405–7415.
- [20] G. R. Hoffman, N. Nassar, R. A. Cerione, *Cell* **2000**, 100, 345–356.
- [21] A. W. Norton, S. Hosier, J. M. Terew, N. Li, A. Dhingra, N. Vardi, W. Baehr, R. H. Cote, *J. Biol. Chem.* **2005**, 280, 1248–1256.
- [22] S. Grizot, J. Faure, F. Fieschi, P. V. Vignais, M. C. Dagher, E. Pebay-Peyroula, *Biochemistry* **2001**, 40, 10007–10013.
- [23] T. A. Cook, F. Ghomashchi, M. H. Gelb, S. K. Florio, J. A. Beavo, *Biochemistry* **2000**, 39, 13516–13523.
- [24] G. Dorman, G. D. Prestwich, *Biochemistry* **1994**, 33, 5661–5673.
- [25] F. Kotzby-Hibert, T. Grutter, M. Goeldner, *Mol. Neurobiol.* **1999**, 20, 45–59.
- [26] G. Dormán, G. D. Prestwich, *Trends Biotechnol.* **2000**, 18, 64–77.
- [27] A. A. Siddiqui, J. R. Garland, M. B. Dalton, M. Sinensky, *J. Biol. Chem.* **1998**, 273, 3712–3717.
- [28] M. Wagner, J. Kuhlmann, *Methods Mol. Biol.* **2004**, 283, 245–254.
- [29] P. Juhasz, M. T. Roskey, I. P. Smirnov, L. A. Haff, M. L. Vestal, S. A. Martin, *Anal. Chem.* **1996**, 68, 941–946.
- [30] O. N. Jensen, A. Podtelejnikov, M. Mann, *Rapid Commun. Mass Spectrom.* **1998**, 10, 1371–1378.
- [31] A. Mateja, Y. Devedjiev, D. Krowarsch, K. Longenecker, Z. Dauter, J. Otlewski, Z. S. Derewenda, *Acta Crystallogr. D: Biol. Crystallogr.* **2002**, 58, 1983–1991.

Received: April 22, 2008

Published online on October 8, 2008